NASA

Technical Memorandum **78096**

Structure of Current Sheets in Magnetic Holes at 1 A.U.

R. J. Fitzenreiter and L. F. Burlaga

FEBRUARY 1978

National Aeronautics and
Space Administration

Goddard Space Flight Center
Greenbelt, Maryland 20771

STRUCTURE OF CURRENT SHEETS IN MAGNETIC HOLES AT 1 A.U.

by

R. J. Fitzenreiter
L. F. Burlaga
NASA/Goddard Space Flight Center
Laboratory for Extraterrestrial Physics
Greenbelt, MD 20771

TO BE SUBMITTED TO: The Journal of Geophysical Research

ABSTRACT

Current density profiles in several types of interplanetary magnetic holes have been calculated using high-resolution IMP-6 magnetic field data (12.5 vector measurements/s), assuming that the currents flow in planar sheets and that the magnetic field varies only in the direction normal to the sheet. The planarity was verified in four holes which were observed by two suitably spaced spacecraft. The structure of the current sheets ranges from very simple in some holes to very complex in others. Four types of simple magnetic holes are discussed, in which $\underset{\sim}{B}$ varies nearly monotonically on each side of the hole. In two of the holes, $\underset{\sim}{B}$ varies in intensity but not in direction as a result of currents normal to $\underset{\sim}{B}$. In the other two holes, $\underset{\sim}{B}$ changes in both magnitude and direction as a result of currents both normal and parallel to $\underset{\sim}{B}$. The observed structures are found to be qualitatively consistent with the models of Burlaga and Lemaire, which are based on self-consistent solutions of Vlasov's equation and Maxwell's equations. Examples of complex, irregular magnetic holes are also presented, and they are shown to contain multiple, current sheets in which currents flow parallel to one another at various angles with respect to $\underset{\sim}{B}$. There is no model of such magnetic holes at present.

1. INTRODUCTION

Magnetic holes in the solar wind (Turner et al., 1977) are thin ($\sim 10^4$ km), isolated regions of low magnetic field intensity ($|\underset{\sim}{B}| < 1\ \gamma$) imbedded in a background of uniform field with nearly average magnetic field intensity. The direction of the magnetic field may change abruptly by a large amount across a hole, it may vary irregularly, or there may be no change in direction. Solar wind observations at 1 AU have shown that magnetic holes occurred at the rate of about 1.5 per day in the interval March 18 - April 6, 1971, and existed in several different states of the solar wind, i.e., in regions that were characterized by streams, shocks, or waves (Turner et al., 1977). Magnetic holes appear to be discrete solar wind structures with their own physical processes. Holes are a class of current sheets. Because the thickness of holes is on the order of 10 R_L to $\sim 100\ R_L$, where R_L is the proton Larmor radius, they are 'kinetic-scale' phenomena according to the scale classification scheme of Burlaga (1969). Models of several types of magnetic hole current sheets have been presented by Burlaga and Lemaire (1978) based on a kinetic theory of sheaths (Lemaire and Burlaga, 1976). In this theory, magnetic holes are a diamagnetic response of the plasma to a local enhancement in the kinetic pressure. The current is due to the magnetization and gradient drift velocities of protons, and it is assumed to flow in a plane sheet. The sheet is assumed to be an equilibrium structure at rest in the moving reference frame of the solar wind. The magnetic field and plasma pressure are assumed to be uniform along the sheet, i.e., all spatial variations are in the normal direction.

The purpose of this paper is to examine the structure of the current sheets in interplanetary magnetic holes. In Section 2 we use observations from the two spacecraft to show that the current sheets which we could examine in this way were approximately planar over a distance of $\approx$ 30 times their thickness. In Section 3 we show how, for planar current sheets, the currents can be calculated from measurements of $\underset{\sim}{B}(t)$ at one spacecraft when the solar wind velocity is known. We use this method to examine the structure of current sheets in several types of magnetic holes. The structure of magnetic holes ranges from very simple to very complex. We present examples of four types of simple holes in Section 4, and we compare the results with models of Burlaga and Lemaire (1978). Examples of complex holes are presented in Section 5.

2. PLANARITY OF CURRENT SHEETS IN MAGNETIC HOLES

A basic assumption in the diamagnetic theory of current sheets (Lemaire and Burlaga, 1976; Burlaga and Lemaire, 1978) is that the curvature of the sheet is small compared with the thickness. This is also crucial in determining currents from observations by one spacecraft, for one can compute $\nabla \times \underset{\sim}{B}$ from magnetic field observations at one spacecraft if and only if the current sheet is planar. One can test for planarity if the current sheet is observed by two suitably placed spacecraft. The method which we use is to compare the normal, $\hat{z}$, determined from the internal structure of the current sheet observed by one spacecraft with the normal $\hat{n}$ determined from the time interval during which the current sheet would pass from one spacecraft to another if it were planar. The local normal, $\hat{z}$, was obtained from high-resolution magnetic field measurements in the current sheet using the method of Sonnerup (1971), which determines by least squares the direction of a plane about which the scatter of the individual magnetic field vectors is a minimum across the hole. The normal $\hat{n}$ was independently computed from the time delay between two spacecraft using the method of Denskat and Burlaga (1977). Figure 1 shows the current sheet as a plane which moves at the solar wind velocity, $\underset{\sim}{V}$, assumed to be radial and constant. The magnetic field is $\underset{\sim}{B}_1$ on one side of the current sheet and $\underset{\sim}{B}_2$ on the other side. The current sheet is observed by one spacecraft at time t_o and by another spacecraft at a time $t_o + T$. It is assumed that the spacecraft are separated by a distance $|\underset{\sim}{L}|$ which is large compared to the thickness of the current sheet. Denskat and Burlaga (1977) showed that if the current sheet is a plane, then the normal to the plane is given by

$$\hat{n} = \frac{(\underset{\sim}{B}_2 - \underset{\sim}{B}_1) \times \underset{\sim}{L}}{|(\underset{\sim}{B}_2 - \underset{\sim}{B}_1) \times \underset{\sim}{L}|} \qquad (1)$$

where $\underset{\sim}{L} = \underset{\sim}{r}_a - \underset{\sim}{r}_b - \hat{x}\,Vt$ is the vector line segment between the points in the plane measured by the two spacecraft. Equation 1 satisfies the geometrical condition $\hat{n} \cdot \underset{\sim}{L} = 0$, and the additional physical condition $(\underset{\sim}{B}_2 - \underset{\sim}{B}_1) \cdot \hat{n} = 0$ obtained from $\nabla \cdot \underset{\sim}{B} = 0$. Thus, the orientation of the assumed plane is completely determined, provided $(B_2 - \underset{\sim}{B}_1) \nparallel \underset{\sim}{L}$. If the planarity assumption is valid, then $\hat{n}$ and $\hat{z}$ should lie along the same direction; if there is significant curvature in the current sheet, then $\hat{n}$ and $\hat{z}$ should be different.

The magnetic field data from IMP-6 and IMP-5 were examined for magnetic holes observed by both spacecraft during the period March 16 to July 1, 1971. Because of the lower resolution of the IMP-5 experiment (one measurement each 2.56 sec), holes are not as easily detected in the IMP-5 data as in IMP-6 data. For this reason, holes were first identified in the IMP-6 data and then looked for in 20 sec averaged IMP-5 data. For the first 25 days of the selected observing period, we started with the holes identified by Turner et al. (1977) in the 1.28 sec IMP-6 data, and we found no holes for which interplanetary data were available at IMP-5, since IMP-5 was in the magnetosphere most of the time. For the remaining 80 days, we began with the 15 sec averaged IMP-6 data. The criteria for selecting holes observed by both spacecraft were: 1) $B_{min} \lesssim 1\ \gamma$ at IMP-6 and an indication of an intensity depression in the lower resolution data of IMP-5; 2) identification of the same discontinuity in direction of the magnetic field in the two data sets. Using the discontinuity in direction as the primary basis for correlation, the time lag, τ, was measured to

the nearest minute of time. Since holes are discrete, usually isolated phenomena, visually correlating holes in the two data sets should be valid, even though somewhat subjective.

A total of 11 holes were found that could be clearly identified in both data sets. In every case where simultaneous, non-magnetospheric data were available, holes seen at IMP-6 were also seen at IMP-5. For seven of the holes, IMP-5 was close to or within the magnetosheath and the background magnetic field was elevated in intensity and fluctuating. The remaining holes (cases in which the background field was most characteristic of the interplanetary field) are listed in Table I along with the results of the analysis. In each case, the current sheet normal, $\hat{z}$, obtained by the minimum variance analysis at IMP-6, was compared with the sheet normal $\hat{n}$ from equation 1. The angle between $\hat{z}$ and $\hat{n}$ show that differences in the normal directions are of the order of the uncertainties in the analysis. These uncertainties are based on error estimates in the determination of $\hat{z}$ and $\hat{n}$. In two cases, ($\hat{z}$ the sheet normal at IMP-5) was determined by the minimum variance analysis and compared with $\hat{z}$ at IMP-6. The results show that the sheet normals at the two locations are parallel within an uncertainty which is consistent with the assumption of planarity over this distance.

The thickness of the current sheet, ℓ, is obtained from

$$\ell = |V \cos \xi| \, T \qquad (2)$$

where T is the width in seconds of time, V is the solar wind speed and ξ is the angle between $\underset{\sim}{V}$ (assumed to be radial) and the current sheet normal. The longitude and latitude of the normal $\hat{z}$ are given in solar ecliptic coordinates. The thickness of the current sheets and the

separation between observing locations in the sheet, L, are compared in Table I. It can be seen that the minimum length to thickness ratio $(L/\ell)_{min}$ is ~ 20.

The uncertainties in the comparison of $\hat{z}$, $\hat{z}'$, and $\hat{n}$ given in Table I are based on a combination of the errors in determining each normal direction. In each case, the rotation angle, ω, of the magnetic field vector across the sheet is $> 90^{o}$, and the ratio of the intermediate to minimum eigenvalues, λ_2/λ_3 is $\tilde{>} 3$. Based on a numerical error analysis of the minimum variance method by Lepping and Behannon (1978), these are ranges of ω and λ_2/λ_3 for which the plane of the current sheet should be well defined. The quantitative estimate of the error, ε, in the normal direction used here is $\sin \varepsilon \sim (\Delta B_z)_{rms} / B_{mean}$, where $(\Delta B_z)_{rms}$ is the rms fluctuation in the normal field component and B_{mean} is the mean field intensity across the sheet. The errors in $\hat{z}$ and $\hat{z}'$ range from 3^{o} to 10^{o} for the holes in Table I. The error in $\hat{n}$ ranges from 5^{o} to 11^{o} due to the ± 0.5 minute uncertainty in determining the lag time.

The effect of the small curvature in the current sheet corresponding to the uncertainties in the sheet normals can be estimated as follows. The current flow when the sheet is planar is $|J_{plane}| \propto \frac{1}{B}\frac{dp}{dz}$, where $\frac{dp}{dz}$ is the kinetic pressure gradient in the sheath. The contribution to the current flow due to possible curvature of the field lines is $|J_{curv}| \propto \frac{1}{B} P/R$ where p is the kinetic pressure and R is the radius of curvature. In magnetic holes, $\frac{dp}{dz} \sim P/\ell$, where ℓ is the sheath thickness, and therefore $|J_{curv}/J_{plane}| \sim \frac{\ell}{R}$. If the angle of curvature is θ over the distance L along the sheet, then $\frac{1}{R} = \frac{\theta}{L}$ and $|J_{curv}/J_{plane}| \sim \frac{\ell}{L}\theta$. For $L/\ell = 20$ and $\theta = 20^{o} = 0.35$ radian (which is an upper limit to the uncertainty in the

planarity determination), $|J_{curv}/J_{plane}| = 0.02$, and the curvature drift current is negligible. Therefore, the results show that these current sheets are thin, with $L/\ell > 20$, and have no significant curvature over the distance $L \sim 2 \times 10^5$ km $\sim 30\ R_E$ (R_E = radius of the earth).

3. COMPUTATION OF CURRENTS IN CURRENT SHEETS

For the calculations of the current, we assumed that it flows in a uniform, planar sheet, i.e., that the field components vary only in the normal direction across the sheet. The sheet normal was determined by the method of minimum variance discussed in Section 2. The accuracy of the normal is related to the ratio of the intermediate to minimum eigenvalue λ_2/λ_3, as discussed above. The measured field components are transformed to the coordinate system in which the z-axis is along the normal to the sheet and the x-y plane lies in the sheet. In this orthogonal coordinate system the components of Mo $\underset{\sim}{J} = \nabla \times \underset{\sim}{B}$ are $\mu_o J_x = - dB_y/dz$, $\mu_o J_y = dB_x/dz$, and $J_z = 0$, where $\underset{\sim}{J}$ is the current density, $\underset{\sim}{B}$ is the magnetic field and μ_o is the permeability of free space. Since the hole is assumed to be a static structure convected past the spacecraft at the solar wind speed, the normal derivative, $\frac{d}{dz}$, is related to observed time variations by the component of the solar wind speed normal to the current sheet, $V_n = V \cos \xi$, by the equations

$$\mu_o J_x = - \frac{1}{V_n} \frac{dB_y}{dt}, \mu_o J_y = \frac{1}{V_n} \frac{dB_x}{dt}, J_z = 0. \qquad (3)$$

We have computed the derivatives using three consecutive points of the appropriate field component measurements, smoothed by a one second running average. The current densities will be plotted in units of the maximum current density in the hole, $|\underset{\sim}{J}|_{max}$.

For later reference, we recall that the current in a current sheet can be expressed in the form

$$\mu_o \text{ Mo } \underset{\sim}{J} = (\hat{z} \times \hat{B}) \frac{dB}{dz} + \underset{\sim}{B} \frac{d\omega}{dz}, \qquad (4)$$

where $\omega(z)$ is the direction of $\underset{\sim}{B}$ with respect to a line in the current

sheet. This shows that $\underset{\sim}{J}$ flows normal to $\underset{\sim}{B}$ when there is no change in the direction of $\underset{\sim}{B}$, and $\underset{\sim}{J}$ flows parallel to $\underset{\sim}{B}$ when there is no change in the intensity of $\underset{\sim}{B}$.

The quantities referred to above, viz., λ_2/λ_3, ξ, $|\underset{\sim}{J}|_{max}$, and ω, as well as the thickness of the hole, ℓ, in units of the proton Larmor radius R_L are given in Table 2 for each of the events discussed in the following sections. We use R_L = 147 km, corresponding to a mean field in the hole of 2.5γ and a temperature of 7.5×10^{4o}K.

4. CURRENTS IN SIMPLE MAGNETIC HOLES

By simple magnetic holes (antiholes), we mean those in which $B = |\underset{\sim}{B}|$ decreases (increases) monotonically from the ambient value outside the hole to a minimum (maximum) at or near the center of the hole. We can distinguish two classes of such holes: those in which $\underset{\sim}{B}$ does not change direction across the hole, and those in which $\underset{\sim}{B}$ does change direction across the hole. In the former, $\underset{\sim}{J}$ flows normal to $\underset{\sim}{B}$, while in the latter there is a component of $\underset{\sim}{J}$ parallel to $\underset{\sim}{B}$ (see equation 4).

We orient the rectangular coordinate system such that $\hat{x}$ is in the plane of the current sheet and along the direction in which the change in $\underset{\sim}{B}$ is greatest, and $\hat{y}$ forms a right-handed coordinate system. For holes with no rotation of $\underset{\sim}{B}$, $B_y = 0$; for holes with rotation of $\underset{\sim}{B}$, $B_y \neq 0$. We shall discuss four cases: a hole and an antihole with $B_y = 0$, and two holes with $B_y \neq 0$.

a) $B_y = 0$, $B_x < 0$. Linear hole. An example of this type of magnetic hole is given in Figure 2. The magnetic field vector is seen to remain essentially along the negative x- direction as the field magnitude passes through a minimum, $B_{min} < 1.0\gamma$ and returns to its original value of $B \sim 5\gamma$. Since there is no change in direction in this case (ω is only 7 degrees), the minimum variance direction, $\hat{z}$, cannot be uniquely defined by measurements at just one location. However, the plane (y-z) in which the vector field changes are a minimum is determined knowing the direction of maximum variance, $\hat{x}$. In this case ξ is estimated using the relation $\xi = 90^{o} - \cos^{-1}(\hat{x} \cdot \underset{\sim}{V}/V)$.

The components of the current density plotted in Figure 2, J_x and J_y, were calculated from $\mu_o \underset{\sim}{J} = \nabla \times \underset{\sim}{B}$ as described in Section 2. The ordinate

of the current plots in this and subsequent plots is in relative units, normalized to the magnitude of the peak current density for the hole which is given in Table 2. The sensitivity of the current calculation to small scale fluctuations in the field can be seen by the level of fluctuations in J_y on either side of the hole relative to the current inside the hole. Since the field variation is almost entirely in B_x, the current is almost entirely in the J_y component and $\underset{\sim}{J}$ is normal to $\underset{\sim}{B}$. The maximum and minimum of J_x in Figure 2 show that there are two adjacent current layers with oppositely flowing currents. Note that the magnitude of the current density, $|\underset{\sim}{J}| = \sqrt{J_x^2 + J_y^2}$, peaks at the point where the magnitude of the field is changing most rapidly in the hole and is zero at the center of the hole where the field change is zero, in agreement with (4). Also, note that the current density profile is asymmetric with respect to the peak, i.e., it rises sharply near the edge of the hole and falls off more slowly toward the center of the hole.

Both the shape and thickness of the current density distributions across the hole in Figure 2 are correctly predicted by the theory of Burlaga and Lemaire (1978) for a model with similar boundary conditions. The hole width, ℓ, which is approximately twice the thickness of each current sheet is $\sim 26\ R_L$ (Table 2). According to the theory, the current is due to the magnetization and gradient drift velocities of protons, which accounts for each sheet being several Larmor radii thick. The skewness of the current profile is explained by the fact that the Larmor radius inside the hole is greater than outside (R_L inside $> R_L$ outside), giving a broader current layer towards the center of the hole.

b) $B_y \tilde{=} 0$, $B_x > 0$. Linear antihole. As defined by Turner et al. (1977), an antihole differs from a hole in that B increases in an antihole whereas it decreases in a hole. Figure 3 shows an antihole in which $\underset{\sim}{B}$ changes nearly along a line. The J_y current profile for the antihole in Figure 3 closely resembles that for the hole in Figure 2. In both cases, there is a current flowing in the $-\hat{y}$ direction on one side of the hole and a symmetrical current flowing in the $+\hat{y}$ direction on the other side of the hole. However, note that B is along $+\hat{x}$ in the antihole and along $-\hat{x}$ in the hole. Thus, $\underset{\sim}{J} \times \underset{\sim}{B}$ points toward the center of the hole but away from the center of the antihole. This is required for equilibrium, because in a magnetic hole there is an enhancement in the plasma pressure, whereas in an antihole there is a depression in the plasma pressure. The basic features of the antihole described above are reproduced in the model of the antihole in Burlaga and Lemaire (1978).

Figure 3 differs from Figure 2 and from the antihole model of Burlaga and Lemaire in that there is a small but significant change in B_y and a corresponding component of current in the $\hat{x}$ direction, J_x, in one half of the antihole. There is thus a component of $\underset{\sim}{J}$ along $\underset{\sim}{B}$ in that sheath. From the bottom panel in Figure 3 it can be seen that $|\underset{\sim}{J} \cdot \underset{\sim}{B}|_{max} \approx 0.5$ in the current sheet on the right side of the antihole. Equation 4 indicates that there is consequently a small rotation of $\underset{\sim}{B}$ in this part of the antihole. This sheath is thus an example of a current sheet in which the change in $\underset{\sim}{B}$ is intermediate between that in the example of Figure 2 (no rotation) and that in the case to be considered next, in which there is a large rotation of $\underset{\sim}{B}$.

c) $B_y \neq 0$, B_x changes sign. Figure 4 illustrates this case in which $\underset{\sim}{B}$ changes direction by rotating across the magnetic hole. (Note that $B_{min} > 1\gamma$, so it does not satisfy the criterion used by Turner et al. (1977) to select holes; nevertheless, it is the same phenomenon.) At the right of the figure is a plot of the tip of the magnetic field vector as it rotates in the (x-y) plane of the current sheet across the holes. The points labeled 1, 2, and 3 correspond to the edges and center of the hole. Since the plotted points are equally spaced in time (80 msec), the spacing of points indicates how rapidly $\underset{\sim}{B}$ is changing through the sheet; the wider the spacing, the more rapid the rotation of $\underset{\sim}{B}$. It can be seen that the current density peaks at point 2 where the change in direction is greatest. Since the variations in B_y are much smaller than those in B_x, $|J_x| \sim |J_y|$, and $\underset{\sim}{J} \simeq J_y \hat{y}$ as in the cases discussed above. In this case, however, $\underset{\sim}{J}$ does not flow normal to $\underset{\sim}{B}$ since $B_y \neq 0$ ($\underset{\sim}{J} \cdot \underset{\sim}{B} \simeq J_y B_y \neq 0$); there is everywhere a component of $\underset{\sim}{J}$ along $\underset{\sim}{B}$. At the center of the hole, where $B_x = 0$ and $|\underset{\sim}{B}| = B_y \neq 0$, $\underset{\sim}{J} \times \underset{\sim}{B} = -J_y B_x \hat{z} = 0$. Thus, $\underset{\sim}{J}$ is parallel to $\underset{\sim}{B}$ at the center of this hole and this current produces the rotation in $\underset{\sim}{B}$ with no change in $|\underset{\sim}{B}|$, in accordance with (4). This case is in contrast to the linear hole in Figure 2, where there is a double current sheet with oppositely flowing currents that produce a change in $|\underset{\sim}{B}|$ with no change in direction. In the case in Figure 4, there is just one current sheet with maximum current at the point where B_x changes sign.

d) B_y, B_x vary. In this last example of a simple hole, we discuss a magnetic hole across which $\underset{\sim}{B}$ rotates through $\omega = 115^o$ (Table 2) as a

result of changes in both B_x and B_y. The magnetic field observations and the calculated currents are shown in Figure 5. In this case, there are two minima in the magnetic field intensity and two overlapping current sheets. The two maxima in $|\underset{\sim}{J}|$ occur where the change in direction of the field vector is greatest. This can be seen from the plot of B_y versus B_x in Figure 5, where the greatest change occurs at points 2 and 4.

The direction of the current with respect to $\hat{B}$ is given by $\hat{J} \cdot \hat{B}$ in the bottom panel of Figure 5. The plot shows that $\hat{J} \cdot \hat{B} = 1$ at the two minima and the central maximum of $|\underset{\sim}{B}|$ in the middle of the hole indicating that the current is flowing along $\underset{\sim}{B}$ at these points. At all other points within the hole, $|\hat{J} \cdot \hat{B}| < 1$ which means there is a component of $\underset{\sim}{J} \perp \underset{\sim}{B}$, which is necessary to support the gradients in $|\underset{\sim}{B}|$.

5. COMPLEX MAGNETIC HOLES

Case a. Figure 6 shows a magnetic hole in which $\underset{\sim}{B}$ reverses direction by shrinking along a line to nearly zero intensity ($B_{min} = 0.12\gamma$) and then increasing in the opposite direction along that line. This is more complex than the holes discussed above, in that it is asymmetrical and it has three different current sheets (labeled a, b, and c in the bottom panel of Figure 6).

The two outer currents, a and c, flow normal to $\underset{\sim}{B}$. Their difference in magnitude is related to the different gradients in $|\underset{\sim}{B}|$ on the two sides of the hole, the larger current corresponding to the steeper gradient in $|\underset{\sim}{B}|$ in accordance with (4). These outer currents flow in the same direction, in contrast to the linear hole in Figure 2 where the currents flow in opposite directions. The difference is due to the fact that B_x changes sign across the hole in Figure 6, but not in Figure 2. The $\underset{\sim}{J} \times \underset{\sim}{B}$ forces, therefore, are oppositely directed on either side of the hole in each case, as required for equilibrium.

The central current, b, is due to two components of $\underset{\sim}{J}$, one (J_y) normal to the average $\underset{\sim}{B}$ direction, and the other (J_x) parallel to $\underset{\sim}{B}$. J_x is associated with a rotation in $\underset{\sim}{B}$ and is related to a small local deviation of $\hat{B}$ from the $\hat{x}$ direction; i.e., it is due to the fact that the variation of $\underset{\sim}{B}$ is not exactly along a line. Smaller fluctuations in J_x and J_y are associated with other small deviations of $\hat{B}$ from $\hat{x}$.

Case b. Figure 7 shows a very broad hole in which there are irregular fluctuations in the magnitude and direction of $\underset{\sim}{B}$. The $|\underset{\sim}{J}|$ profile shows that there are several current sheets in the hole, and the fact that B_z is close to zero throughout the hole indicates that these current sheets

are nearly parallel to one another. The hole is bounded by two current sheets with relatively large current densities. In one of these sheets (on the right-hand side of the figure), the current flows normal to $\underset{\sim}{B}$, while in the other there is a component of $\underset{\sim}{J}$ along $\underset{\sim}{B}$ as well as normal to $\underset{\sim}{B}$. The other current sheets are associated with irregular fluctuations in the direction and magnitude of $\underset{\sim}{B}$. Note that in one part of the hole $|\underset{\sim}{B}| = 0$ for a few seconds and $|\underset{\sim}{J}|$ is zero there. It is conceivable that one could model complex magnetic holes such as this by modeling each of the current sheets separately using the stationary equilibrium theory of Burlaga and Lemaire (1978) and setting them side by side. However, it is also possible that such complex magnetic holes are not in equilibrium and are not stationary. Observations by at least two spacecraft are needed in order to distinguish these two alternatives.

Case c. We conclude by discussing a rare structure which is suggestive of an unstable hole. The unique feature of this "hole", shown in Figure 8, is the presence of nearly periodic oscillations in $|\underset{\sim}{B}|$. The amplitude of the oscillations is largest near the center of the hole, where the direction of $\underset{\sim}{B}$ changes most rapidly, and it decreases to zero with increasing distance from the center of the hole. Calculating $\underset{\sim}{J}$ as we did for the other events discussed in this paper, we find one large peak in $|\underset{\sim}{J}|$, associated with the large change in the direction of $\underset{\sim}{B}$ at the center of the hole, and several secondary peaks on each side. The primary maximum in $|\underset{\sim}{J}|$ is probably significant, since $B_z = 0$ in that current sheet. The secondary maxima, however, do not necessarily represent secondary current sheets, since the assumption of planarity is not satisfied across this "hole", as indicated by the fluctuations in B_z. The oscillations in $|\underset{\sim}{B}|$ suggest

the presence of an instability associated with the central current sheet. This could be driven by changes in conditions across the current sheet (e.g., by a velocity shear) or by currents in the current sheet itself. There are no plasma data with sufficient time resolution to investigate these mechanisms quantitatively.

6. SUMMARY

We have calculated the current density profiles in several types of interplanetary magnetic holes assuming that the current flows in planar sheets and that the variation in the field is normal to the sheet. The validity of the planarity assumption and a lower limit on the extent of the current sheet were determined in four holes observed simultaneoulsy by two separated spacecraft. The distance L between the points on the sheet sampled by each spacecraft was $\sim 30\ R_E$. We found the current sheets to be thin, with the minimum length to sheet thickness ratio $L/\ell = 20\text{-}150$. In each case, we found that the angle of curvature over the distance L was less than 20^o (the order of the uncertainty in the analysis), and that this amount of curvature would contribute negligibly to the drift currents in the sheet. Thus, planarity was verified in these four current sheets, the only events that could be observed in this way in the selected data interval.

The internal structures of four types of simple current sheets were presented, in which the magnetic field intensity varied nearly monotically on each side of the hole. In two cases (one was an antihole), the magnetic field vector $\underset{\sim}{B}$ varied along a line with no rotation and the current density $\underset{\sim}{J}$ was essentially perpendicular to $\underset{\sim}{B}$. The current sheets were double layered with oppositely flowing currents in each layer such that the $\underset{\sim}{J} \times \underset{\sim}{B}$ forces balanced the pressure gradients on each side of the hole. Two cases were presented in which there was a rotation in $\underset{\sim}{B}$ as well as a change in field intensity. In these cases there were two components of $\underset{\sim}{J}$, one parallel to $\underset{\sim}{B}$ which caused the rotation, and the other perpendicular to $\underset{\sim}{B}$ which supported the gradient in $|\underset{\sim}{B}|$. The profiles of these simple type current sheets were shown to be qualitatively consistent with the

theoretical models of magnetic holes by Burlaga and Lemaire (1978). The magnitude of the current density and the sheet thickness are also in quantitative agreement with the theory: $|\underset{\sim}{J}|_{max} \sim 10^{-8}$ amperes m^{-2} and $\ell \sim$ several proton Larmor radii. Examples of current sheets were also discussed which have a more complex internal structure, i.e., irregular variations in intensity and direction of $\underset{\sim}{B}$. Two of these holes were shown in which there were multiple current sheets with components of $\underset{\sim}{J}$ with parallel and perpendicular to $\underset{\sim}{B}$ and which flowed in planes parallel to one another.

A fundamental assumption in both the theory of holes and in the interpretation of the observations in that these current sheets are static structures convected along with the solar wind. A final example was presented in which the plane of the current sheet was not well defined across the hole and the variation in $\underset{\sim}{B}$ was oscillatory, suggestive of an instability in the sheet.

ACKNOWLEDGMENTS

We thank Drs. N. F. Ness and D. Fairfield for making possible the use of the IMP-5 and IMP-6 GSFC magnetometer data for this investigation. We appreciate the help of Dr. K. Behannon, who provided valuable assistance regarding the minimum variance analysis technique. We acknowledge the programming assistance of Mr. L. Klein and discussions with him on the current density calculations.

REFERENCES

Burlaga, L. F., Directional discontinuities in the interplanetary magnetic field, Solar Phys., 7, 54, 1969.

Burlaga, L. F., and J. F. Lemaire, Interplanetary magnetic holes: theory, J. Geophys. Res. (submitted), 1978.

Denskat, J., and L. F. Burlaga, Multispacecraft observations of microscale fluctuations in the solar wind, J. Geophys. Res., 82, 2693, 1977.

Lemaire, J. F., and L. F. Burlaga, Diamagnetic boundary layers in the solar wind: a kinetic theory, Astrophys. and Space Sci., 45, 303, 1976.

Lepping, R. P., and K. W. Behannon, Magnetic field directional discontinuities: an error analysis, to be published, 1978.

Sonnerup, B. U. O., Magnetopause structure during the magnetic storm of September 24, 1961, J. Geophys. Res., 76, 6717, 1971.

Turner, J. M., L. F. Burlaga, J. F. Lemaire, and N. F. Ness, Magnetic holes in the solar wind, J. Geophys. Res., 82, 1921, 1977.

TABLE 1

RESULTS OF TWO-SPACECRAFT OBSERVATIONS OF MAGNETIC HOLES

1971	April 19		May 3		April 13		June 28	
S/C: IMP	6	5	6	5	6	5	6	5
t_o (UT)	0439		1409		0836		0856	
τ (min)		10.5		0		10.0		-2.5
ω (deg)	138		92	99	143	137	161	
λ_2/λ_3	16.2		10.4	8.8	3.1	2.6	3.1	
$\hat{z}$: (ϕ, θ)	(338,32)		(12,6)		(336,60)		(4, -9)	
$\cos^{-1}(\hat{z}.\hat{n})$ (deg)	10 ± 12		18 ± 9		13 ± 17		6 ± 10	
$\cos^{-1}(\hat{z}.\hat{z}')$ (deg)			13 ± 6		16 ± 10			
ℓ (km)	1540		12700		4010		7470	
L (km)	2.33×10^5		2.61×10^5		2.55×10^5		1.87×10^5	
$\frac{L}{\ell}$	150		21		64		25	

TABLE 2

CHARACTERISTICS OF CURRENT SHEETS WHOSE INTERNAL STRUCTURE IS SHOWN IN FIGURES 2 THROUGH 8

UT Date (1971)	ω (deg)	$\frac{\lambda_2}{\lambda_3}$	Hole Width (sec)	V (km/s)	cos ξ	Hole Width ℓ (km)	$\frac{\ell}{R_L}$	$\left\|J\right\|_{max}$ $\left(10^{-9} \frac{\text{amperes}}{\text{m2}}\right)$
1633 March 24	7	1.9	10	501	0.756	3790	26	4.82
0549 March 23	13	5.2	7	316	0.943	2090	14	9.92
1215 April 5	94	18.0	2	514	0.858	882	6	10.49
1349 March 27	116	4.3	7	488	0.518	1770	12	5.86
0440 March 27	169	2.0	6	529	0.994	3150	21	16.38
0308 April 3	37	8.8	17	357	0.864	5240	36	6.51
2116 March 30	64	1.5	13	346	0.927	4170	28	10.12

FIGURE CAPTIONS

Figure 1 Sketch illustrating the two spacecraft analysis technique (after Denskat and Burlaga, 1977).

Figure 2 A linear hole in which $B_y = 0$, $B_x < 0$ (no rotation) across the hole. The current sheet is double layered with $\underset{\sim}{J}$ in opposite directions in each layer and perpendicular to $\underset{\sim}{B}$.

Figure 3 A linear "antihole" in which $B_y \approx 0$, $B_x > 0$. It is physically similar to the linear hole in Figure 2.

Figure 4 Current sheet in which there is a rotation, $\omega = 94^o$ ($B_y \approx$ constant $\neq 0$, B_x changes sign). There is a single current density peak in which $\underset{\sim}{J}$ is predominantly parallel to $\underset{\sim}{B}$ and a small component of $\underset{\sim}{J}$ is perpendicular to to $\underset{\sim}{B}$.

Figure 5 Current sheet in which $\underset{\sim}{B}$ rotates, $\omega = 116^o$ (B_y varies, B_x changes sign). In this case there are two overlapping current layers.

Figure 6 Complex hole in which there are three current layers parallel to one another ($B_z = 0$). This is an example in which $\underset{\sim}{B}$ changes along a line, shrinking to ≈ 0 and reversing direction.

Figure 7 Complex hole consisting of multiple, parallel current sheets.

Figure 8 Structure resembling a hole but with oscillatory variations in $|\underset{\sim}{B}|$ suggestive of an instability. Note that $B_z \neq 0$ across the hole indicating that the current sheet may not be well defined for this case.

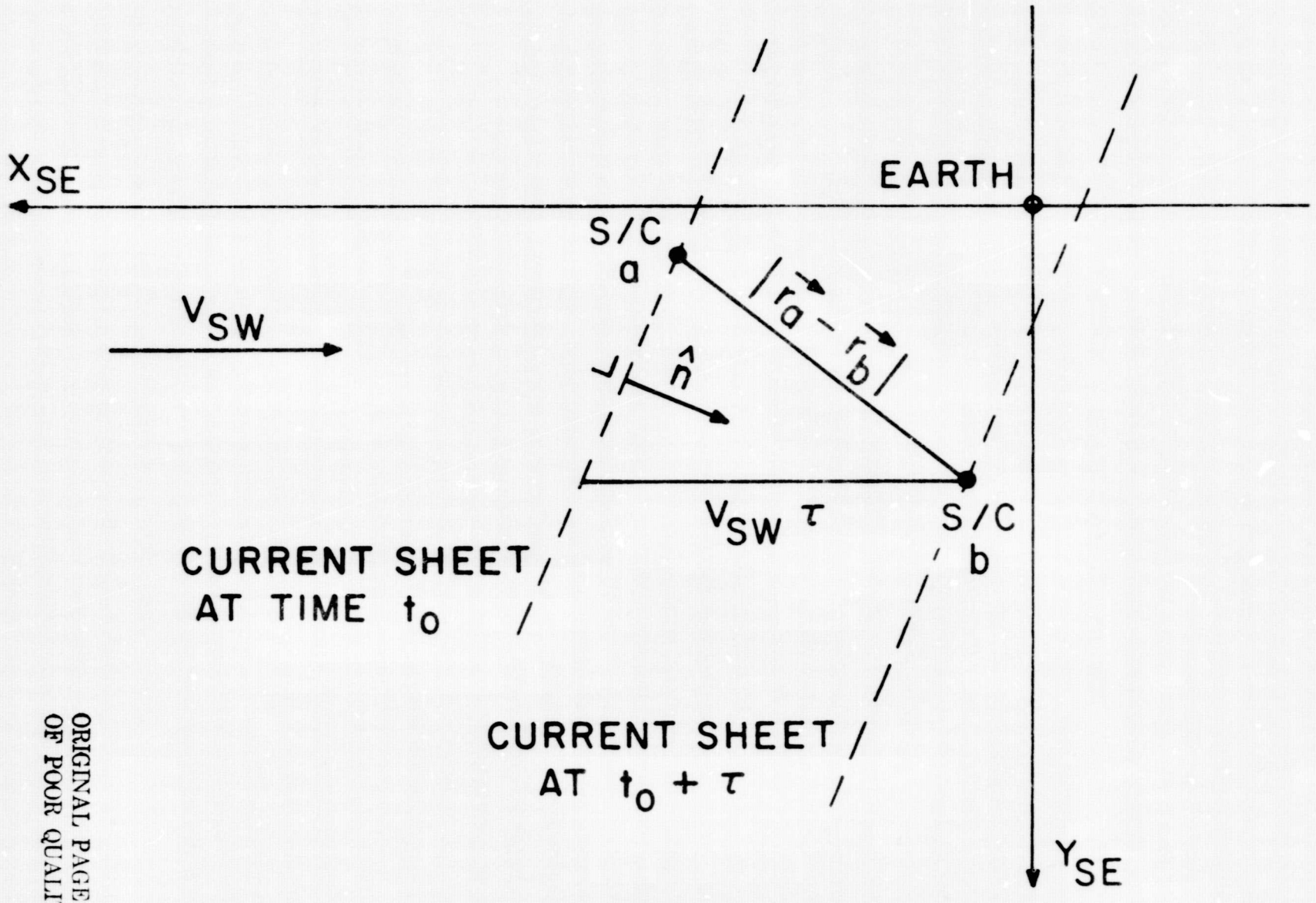

Figure 1

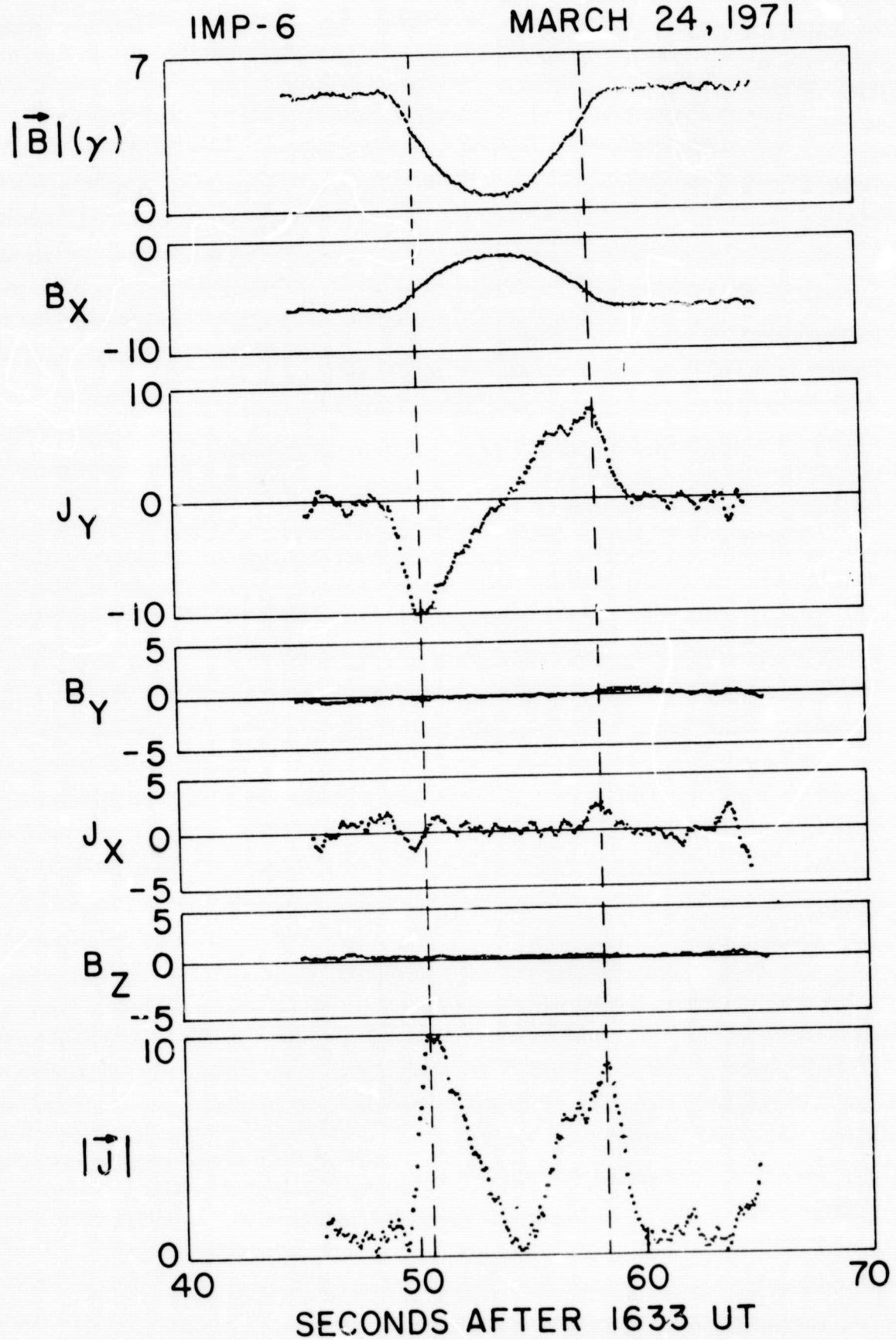
IMP-6
MARCH 24, 1971
|B| (γ)
7
0
B_X
0
-10
J_Y
10
0
-10
B_Y
5
0
-5
J_X
5
0
-5
B_Z
5
0
-5
|J|
10
0
40
50
60
70
SECONDS AFTER 1633 UT

Figure 2

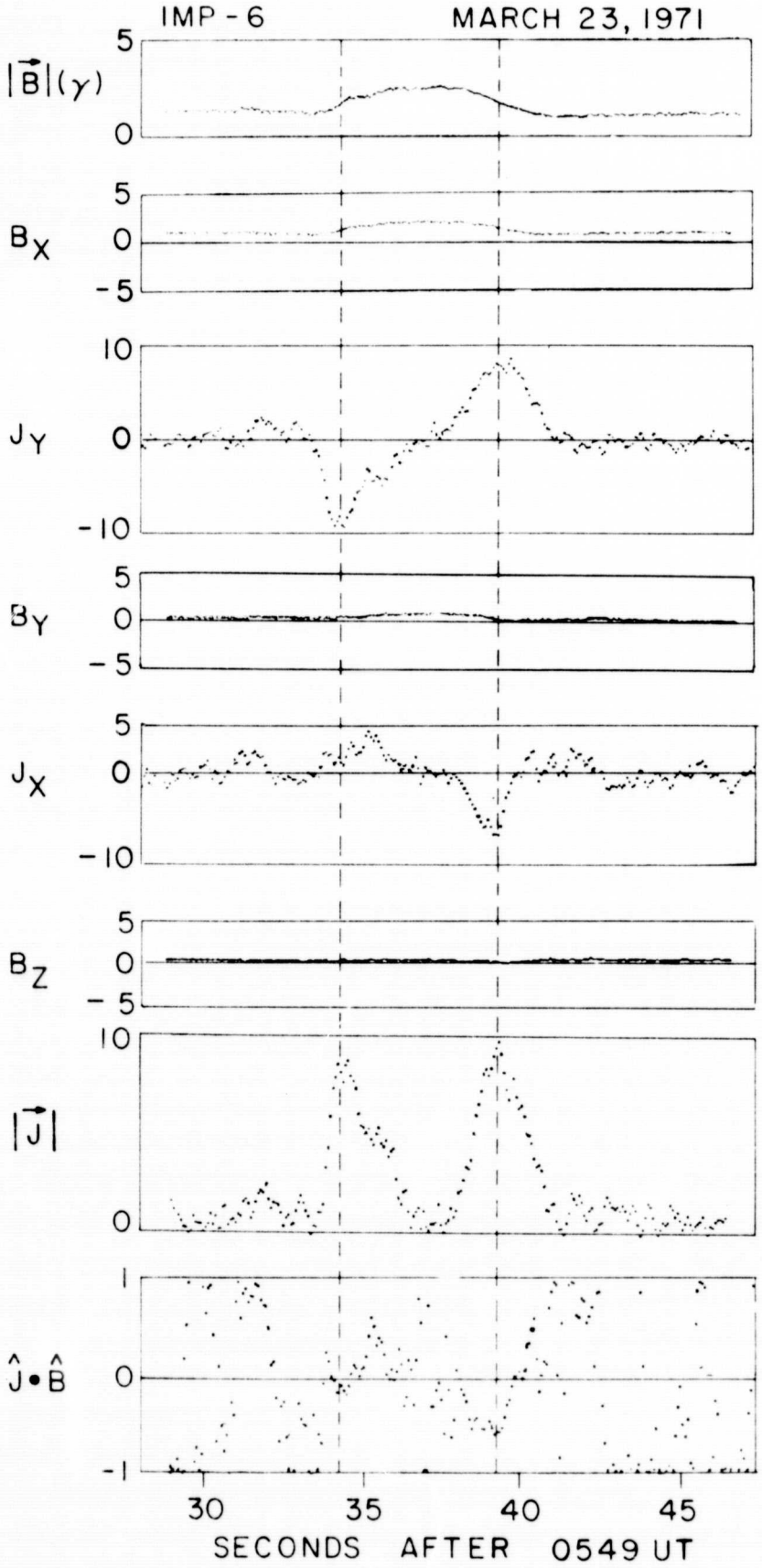

Figure 3

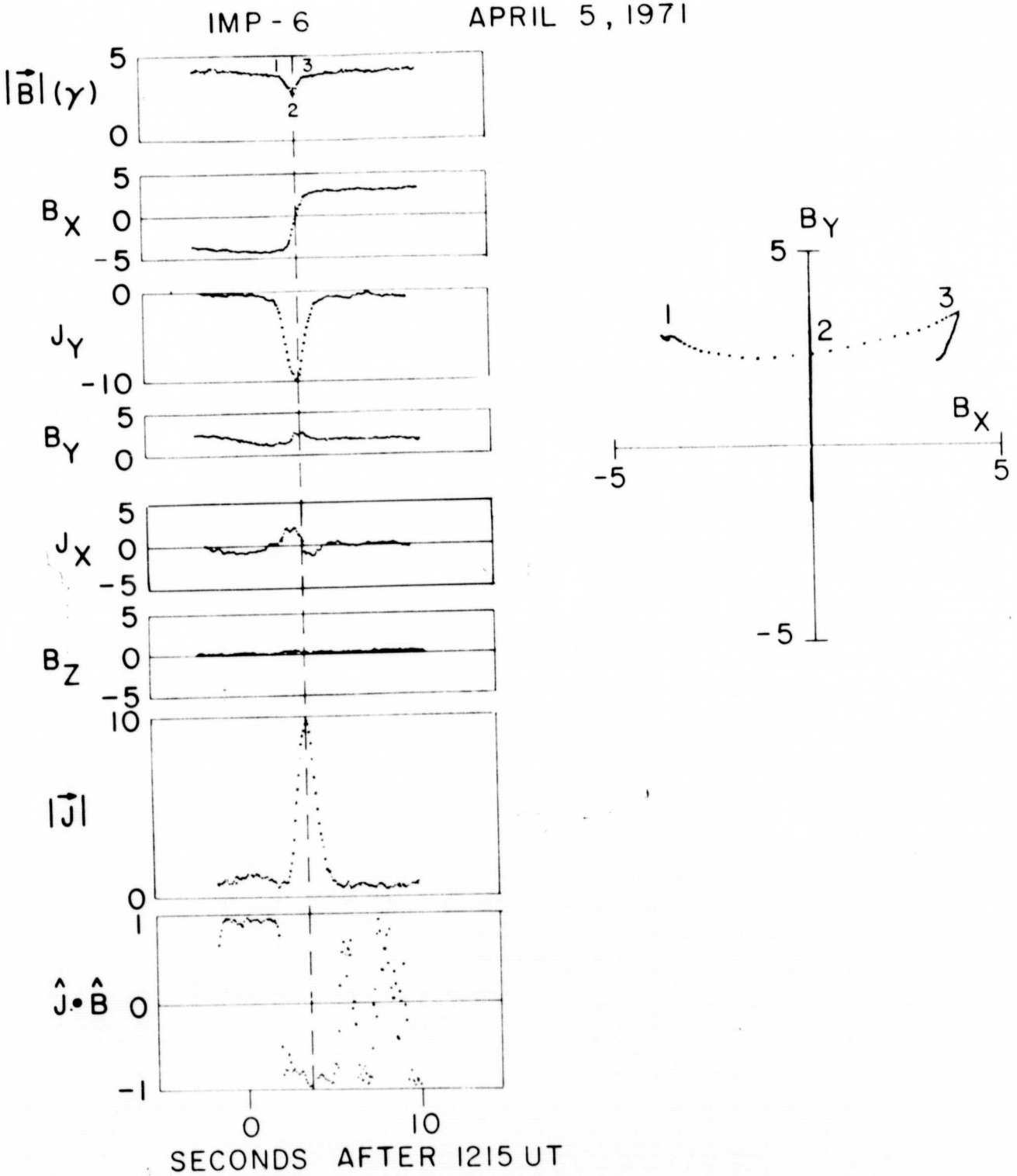
IMP - 6
APRIL 5, 1971
|B| (γ)
B_X
J_Y
B_Y
J_X
B_Z
|J|
Ĵ•B̂
1
2
3
SECONDS AFTER 1215 UT
B_Y
B_X

Figure 4

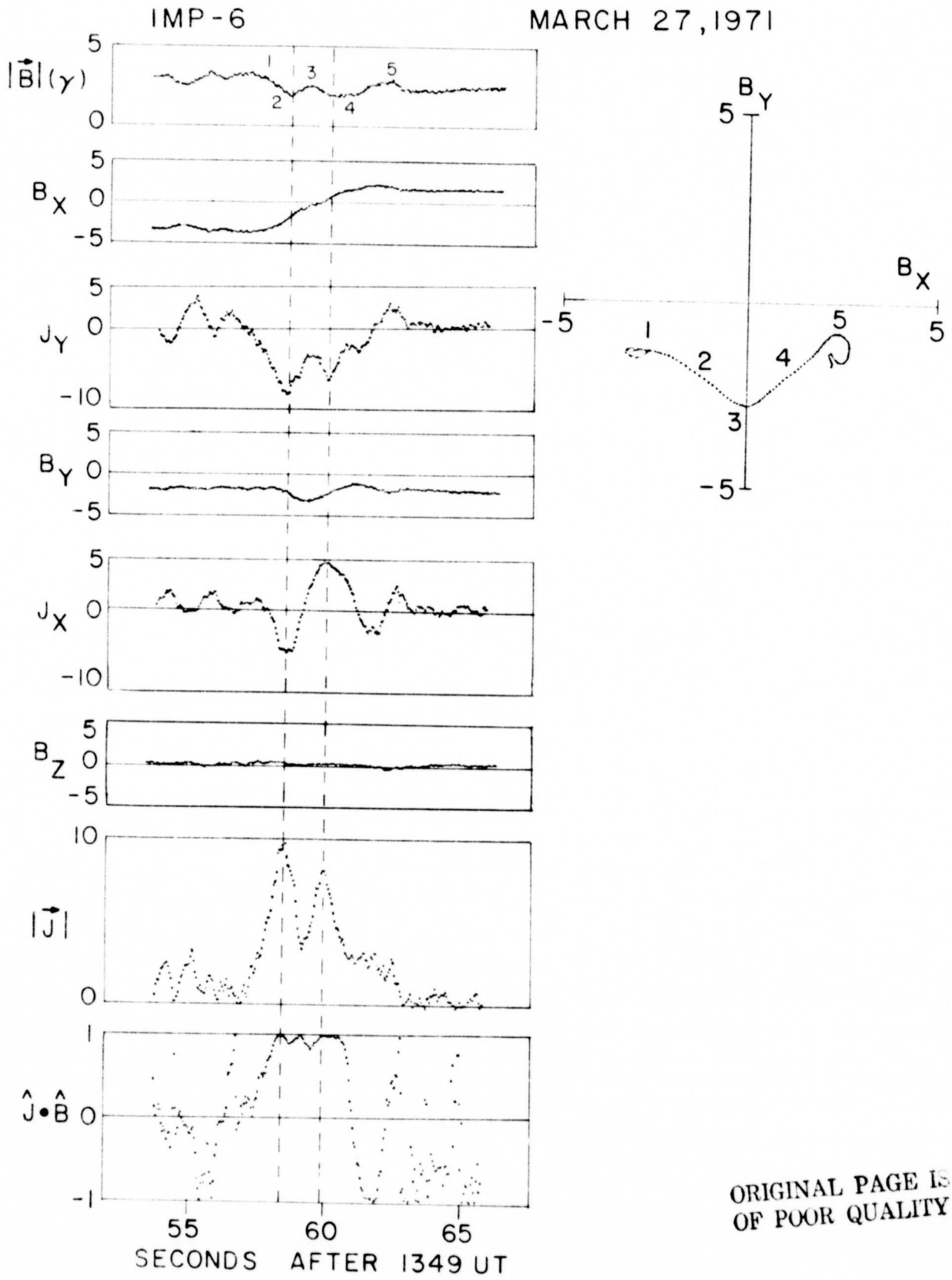

ORIGINAL PAGE IS
OF POOR QUALITY

Figure 5

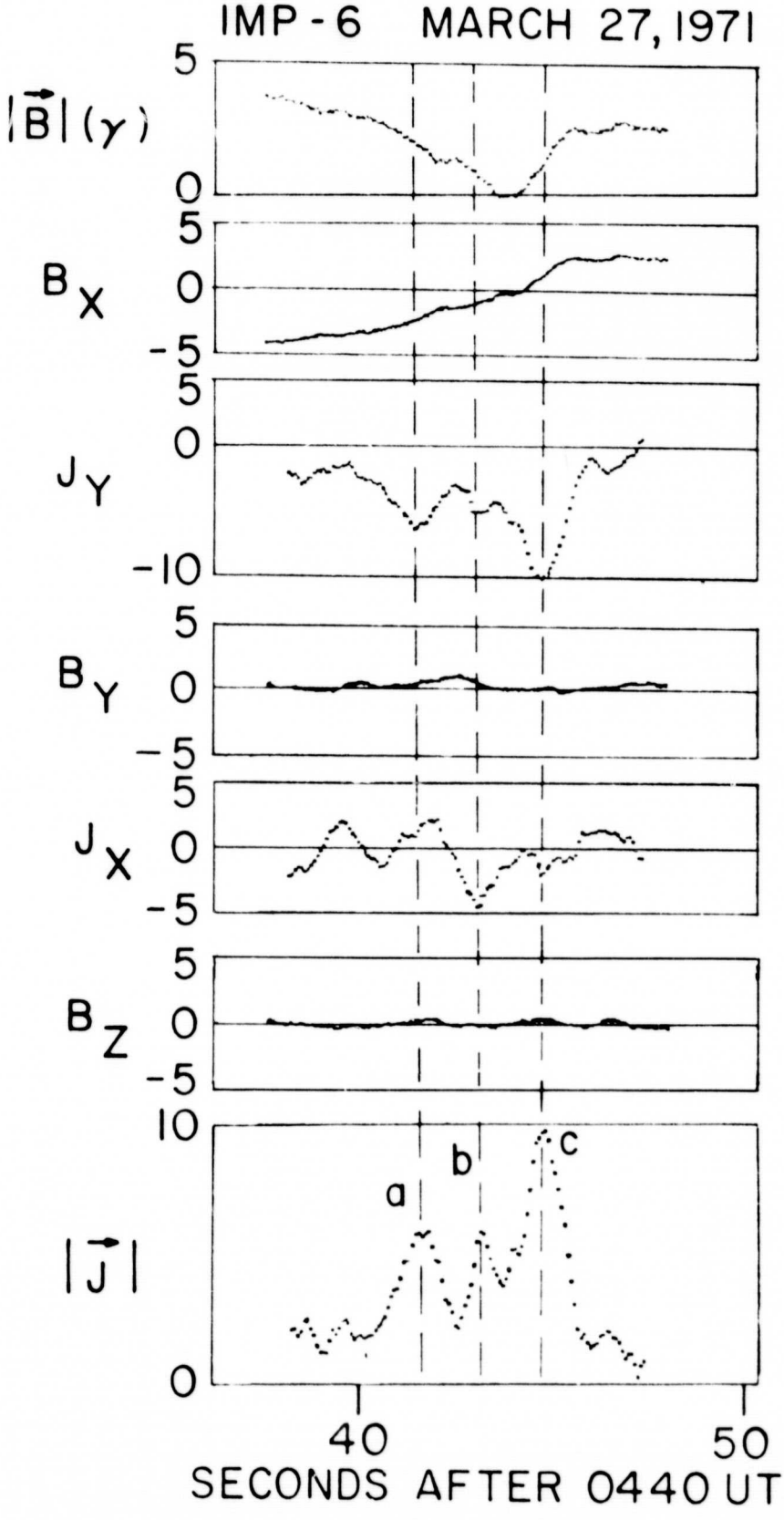
IMP - 6 MARCH 27, 1971
|B| (γ)
5
0
B X
5
0
-5
J Y
5
0
-10
B Y
5
0
-5
J X
5
0
-5
B Z
5
0
-5
|J|
10
0
a
b
c
40
50
SECONDS AFTER 0440 UT

Figure 6

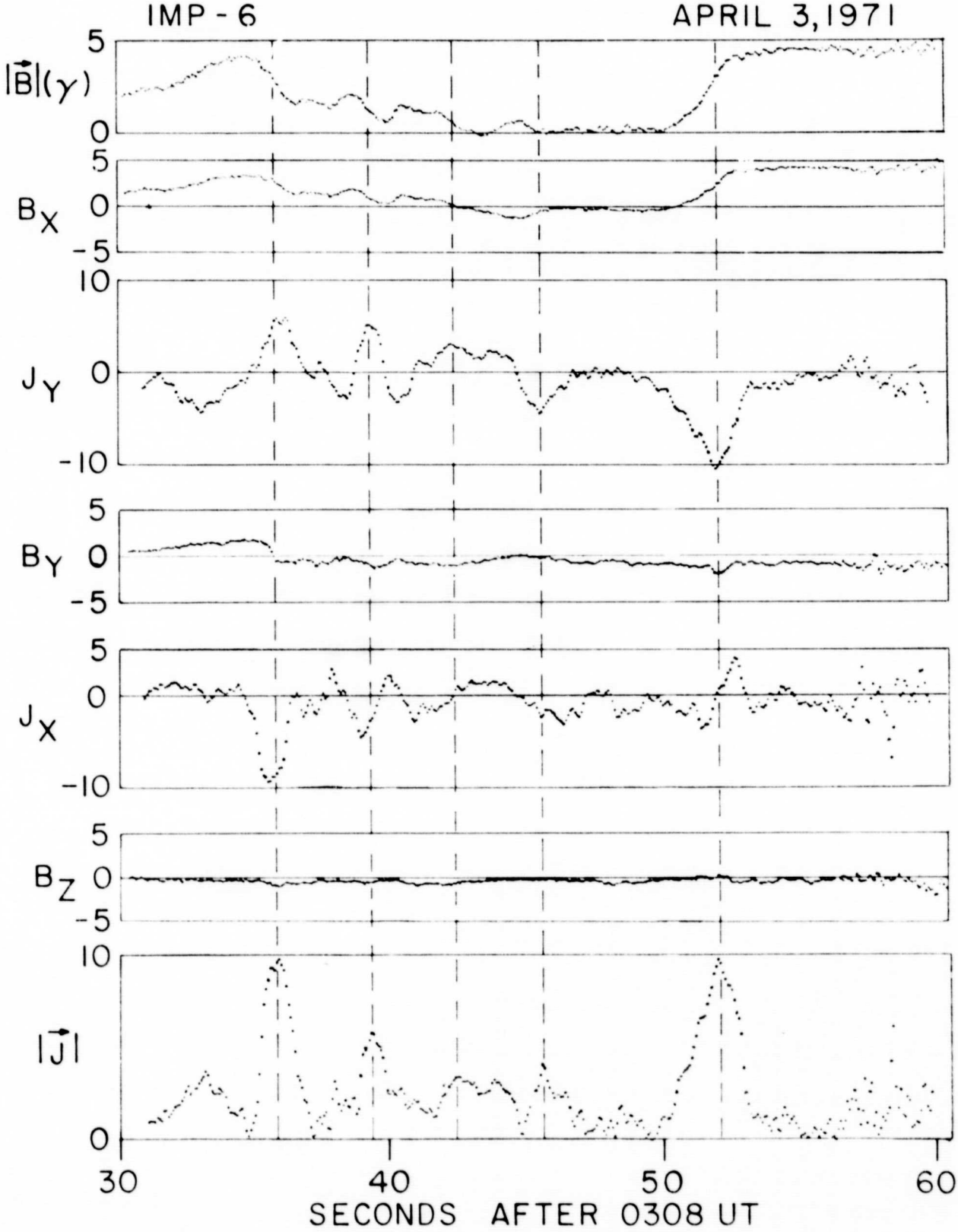

Figure 7

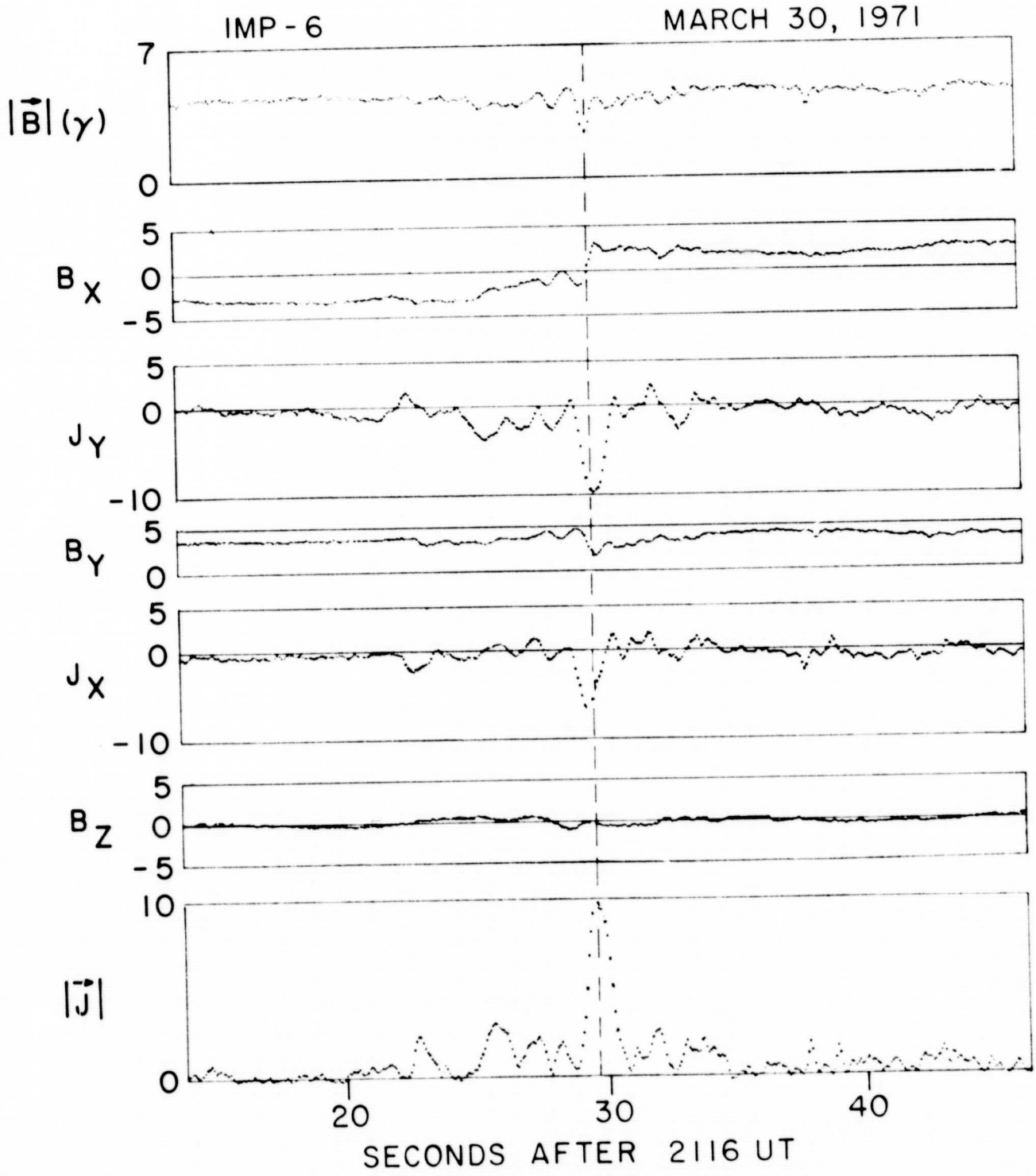
IMP - 6
MARCH 30, 1971
|B| (γ)
7
0
B X
5
0
-5
J Y
5
0
-10
B Y
5
0
J X
5
0
-10
B Z
5
0
-5
|J|
10
0
20
30
40
SECONDS AFTER 2116 UT

Figure 8

BIBLIOGRAPHIC DATA SHEET

1. Report No.	2. Government Accession No.	3. Recipient's Catalog No.
TM-78096		

4. Title and Subtitle	5. Report Date
Structure of Current Sheets in Magnetic Holes at 1 A. U.	February 1978
	6. Performing Organization Code
7. Author(s)	8. Performing Organization Report No.
R. J. Fitzenreiter and L. F. Burlaga	
9. Performing Organization Name and Address	10. Work Unit No.
NASA/GSFC Laboratory for Extraterrestrial Physics Interplanetary Physics Branch, Code 692 Greenbelt, MD 20771	11. Contract or Grant No.
	13. Type of Report and Period Covered
12. Sponsoring Agency Name and Address	Technical Memorandum
	14. Sponsoring Agency Code

15. Supplementary Notes

16. Abstract Current density profiles in several types of interplanetary magnetic holes have been calculated using high-resolution IMP-6 magnetic field data (12.5 vector measurements/s), assuming that the currents flow in planar sheets and that the magnetic field varies only in the direction normal to the sheet. The planarity was verified in four holes which were observed by two suitably spaced spacecraft. The structure of the current sheets ranges from very simple in some holes to very complex in others. Four types of simple magnetic holes are discussed, in which $\underset{\sim}{B}$ varies nearly monotonically on each side of the hole. In two of the holes, $\underset{\sim}{B}$ varies in intensity but not in direction as a result of currents normal to $\underset{\sim}{B}$. In the other two holes, $\underset{\sim}{B}$ changes in both magnitude and direction as a result of currents both normal and parallel to $\underset{\sim}{B}$. The observed structures are found to be qualitatively consistent with the models of Burlaga and Lemaire, which are based on self-consistent solutions of Vlasov's equation and Maxwell's equations. Examples of complex, irregular magnetic holes are also presented, and they are shown to contain multiple, current sheets in which currents flow parallel to one another at various angles with respect to $\underset{\sim}{B}$. There is no model of such magnetic holes at present.

17. Key Words (Selected by Author(s))	18. Distribution Statement
Interplanetary magnetic holes, current sheets	

19. Security Classif. (of this report)	20. Security Classif. (of this page)	21. No. of Pages	22. Price*
U	U	33	

*For sale by the National Technical Information Service, Springfield, Virginia 22151.